Stem Cell Research (2013) 11, 1206–1221

Available online at www.sciencedirect.com

ScienceDirect

www.elsevier.com/locate/scr

Stepwise, non-adherent differentiation of human pluripotent stem cells to generate basal forebrain cholinergic neurons *via* hedgehog signaling

Lucy A. Crompton[a], Meg L. Byrne[a], Hannah Taylor[a], Talitha L. Kerrigan[a], Gilles Bru-Mercier[a], Jennifer L. Badger[a], Peter A. Barbuti[a], Jihoon Jo[a], Sue J. Tyler[a], Shelley J. Allen[a], Tilo Kunath[b], Kwangwook Cho[a], Maeve A. Caldwell[a,*]

[a] *Henry Wellcome Laboratory for Integrative Neuroscience and Endocrinology, School of Clinical Sciences, University of Bristol, Dorothy Hodgkin Building, Whitson Street, Bristol BS1 3NY, UK*
[b] *MRC Centre for Regenerative Medicine, Institute for Stem Cell Research, University of Edinburgh, Edinburgh EH9 3JQ, UK*

Received 7 January 2013; received in revised form 12 July 2013; accepted 2 August 2013
Available online 9 August 2013

Abstract Basal forebrain cholinergic neurons (bfCNs) which provide innervation to the hippocampus and cortex, are required for memory and learning, and are primarily affected in Alzheimer's Disease (AD), resulting in related cognitive decline. Therefore generation of a source of bfCNs from human pluripotent stem cells (hPSCs) is crucial for *in vitro* disease modeling and development of novel AD therapies. In addition, for the advancement of regenerative approaches there is a requirement for an accurate developmental model to study the neurogenesis and survival of this population. Here we demonstrate the efficient production of bfCNs, using a novel embryoid body (EB) based non-adherent differentiation (NAdD) protocol. We establish a specific basal forebrain neural stem cell (NSC) phenotype *via* expression of the basal forebrain transcription factors NKX2.1 and LHX8, as well as the general forebrain marker *FOXG1*. We present evidence that this lineage is achieved *via* recapitulation of embryonic events, with induction of intrinsic hedgehog signaling, through the use of a 3D non-adherent differentiation system. This is the first example of hPSC-derived basal forebrain-like NSCs, which are scalable *via* self-renewal in prolonged culture. Furthermore upon terminal differentiation these basal forebrain-like NSCs generate high numbers of cholinergic neurons expressing the specific markers ChAT, VAChT and ISL1. These hPSC-derived bfCNs possess characteristics that are crucial in a model to study AD related cholinergic neuronal loss in the basal forebrain. Examples are expression of the therapeutic target $p75^{NTR}$, the release of acetylcholine, and demonstration of a mature, and functional electrophysiological profile. In conclusion, this work provides a renewable source of human functional bfCNs applicable for studying AD specifically in the cholinergic system, and also provides a model of the key embryonic events in human bfCN development.

* Corresponding author. Fax: +44 117 331 3169.
E-mail address: Maeve.Caldwell@Bristol.ac.uk (M.A. Caldwell).

1873-5061/$ - see front matter
http://dx.doi.org/10.1016/j.scr.2013.08.002

Introduction

AD is the most common age-related neurodegenerative disease estimated to affect approximately 30 million people worldwide (Holtzman et al., 2011). Most prevalent symptoms are confusion and memory loss caused by synaptic dysfunction and neuronal death. One of the primary neuronal populations affected are the bfCNs, which are partly responsible for these cognitive deficits (Holtzman et al., 2011; Everitt and Robbins, 1997).

The progress of AD research has been inhibited by lack of accurate models that recapitulate the complex facets of AD (Han et al., 2011). Recent advances in hPSC technology have made it possible to produce regionally specified neuronal populations affected by various neurodegenerative conditions, providing a novel source of human neurons for *in vitro* disease modeling (Nat and Dechant, 2011; Liu, 2011). It is essential that these neurons are phenotypically accurate and functional, and that they can also be used to model the embryonic differentiation of these populations, which is applicable to their regenerative potential (Liu, 2011).

Previous studies have demonstrated the generation of cholinergic neurons, with a potential basal forebrain phenotype (Nilbratt et al., 2010; Bissonnette et al., 2011). However, high levels of specific extrinsic factors were used to direct differentiation, of which their exact role remains unclear. Our aim was to provide a method of generating high numbers of bfCNs in keeping with a requirement for a developmental model; a reductionist approach, where the cells establish their own developmental cues, in parallel to the developing embryo. Our reasoning for the advantages of this are two-fold; firstly we believe this approach provides a superior and more accurate developmental model to study the innate acquisition of basal forebrain cholinergic fate; furthermore by using intrinsic cues from development we would suggest that the resulting neuronal progeny would be more similar to those in the developing brain. We present evidence that a method of EB-based non-adherent differentiation (NAdD) is sufficient for the induction of basal forebrain fate. In the embryo, bfCNs differentiate in the ventral telencephalon, which will go on to form part of the basal forebrain (Marin et al., 2000). Hedgehog signaling is the master controller of dorso-ventral patterning, inducing ventral fate along the entire length of the developing neural tube (Briscoe and Ericson, 1999). We show that NAdD results in the production of the secreted hedgehog ligand SHH, which as in the embryonic ventral telencephalon, results in expression of the specific transcription factors NKX2.1 and *LHX8* (Marin et al., 2000; Ericson et al., 1995a; Shimamura et al., 1995; Pera and Kessel, 1997; Gunhaga et al., 2000; Sussel et al., 1999; Flandin et al., 2010; Zhao et al., 2003; Fragkouli et al., 2005). Optimization of the NAdD protocol generated an expandable population of NKX2.1$^+$/LHX8$^+$ NSCs, which retained this phenotype through long-term expansion. Upon terminal differentiation the NSCs generated TUJ1$^+$/ChAT$^+$ cholinergic neurons, demonstrating characteristics of bfCNs present in the adult human brain. Briefly they expressed high levels of p75^{NTR} protein, as well as cholinergic receptor subunit genes, essential for their function and upon transplantation the NSCs were also able to differentiate into cholinergic neurons in the adult rat brain. Furthermore, the hPSC-derived bfCNs were electrically active, released acetylcholine, and generated neuronal action potential firing as well as spontaneous activity. Therefore our work provides a model of the human bfCN population, which meets the criteria required for a multipurpose model of the basal forebrain cholinergic system, both developmentally and also in a mature functional context.

Materials and methods

hPSC culture

Shef hES lines were originally acquired from the UK-Stem Cell Bank. The NAS2 hiPS cell line was generated as previously described (Devine et al., 2011). The MSU0001 hiPS cells were a kind gift from Dr Jose Bernado Cibelli, Cellular Reprogramming Laboratory, Michigan State University (Ross et al., 2010). Cells were maintained upon mitotically inactivated mouse embryonic fibroblasts in growth media (80% KO-DMEM, 20% Knock-out Serum Replacer (KSR), 1% non-essential amino acids, 2 mM Glutamax, 0.1 mM ß-Mercaptoethanol, and 1% penicillin and streptomycin all Life Technologies), supplemented with either 10 ng/ml (Shef hES and NAS2 hiPS) or 20 ng/ml (MSU0001) FGF2 (Peprotech). Cells were passaged manually.

Neural differentiation optimized for generation of basal forebrain progenitors

A minimum of six 5 cm plates, containing approximately 25 colonies each were required to provide an adequate number of cells. Cells were washed with KO-DMEM (Life Technologies) and incubated in 1 mg/ml Collagenase IV (Life Technologies) for 30 min at 37 °C. Whole-colonies were remove and centrifuged at 50 ×*g* for 5 min. Colonies were chopped into uniform 150 μm pieces using a McIlwain tissue chopper (Mickle Engineering, Gomshall, U.K.), and resuspended in growth media (described above), without FGF2 but supplemented with 10 μM of the ROCK inhibitor Y27632 (Tocris). The pieces were transferred to a 25 cm (Everitt and Robbins, 1997) flask, coated with poly(2-hydroxyethyl methacrylate) (Sigma) to prevent cell attachment. Colony pieces formed spheres and differentiated into EBs over 4 subsequent days, after which they were transferred into modified chemically defined media (CDM) (Joannides et al., 2007), (BSA was substituted with 400 μg/ml Albumax-II, Life Technologies). CDM was supplemented with 10 μM Y27632 (Tocris) and 20 μM of the Nodal/TGF-β signaling inhibitor SB431542 (Tocris). During this period of neural enrichment EBs were regularly triturated with P1000 tip to prevent aggregation. After 8 days the neurospheres were transferred into NEM (7 parts KO-DMEM to 3 parts F12, 2 mM Glutamax, 1% penicillin and streptomycin, supplemented with 2% B27 (all Life Technologies), plus FGF2 and EGF [20 ng/ml] and heparin [5 μg/ml]) (Svendsen et al., 1998). NEM also contained 20 μM SB431542 and 10 μM Y27632, for the initial 10 day expansion period. We found that regular trituration of the EBs throughout enrichment, and passaging using the McIlwain tissue chopper (Mickle Engineering, Gomshall, U.K.) at day 10 of expansion were crucial to achieve a pure population of NSCs. Neurospheres were passaged every 2 weeks by chopping them into 200 μm pieces (Svendsen et al., 1998) (Anderson et al., 2007).

For monolayer differentiation hPSCs were seeded on Matrigel coated plastic-ware and differentiated as described (Chambers et al., 2009).

Acute, single cell plate-downs for NSC counts

Neurospheres were dissociated using Accutase (Sigma) and resuspended in NEM without mitogens. 50,000 NSCs were plated on each PDL/laminin coated coverslip. For NESTIN/MSI1 counts cells were left for 12 h prior to fixation. Other plating times are detailed in the Results section.

Whole neurosphere terminal differentiation for iummunocytochemistry

Whole neurospheres were plated on PDL/laminin coated coverslips in NEM and allowed to differentiate for 28 days (Caldwell et al., 2001).

Semi-quantitative RT-PCR

Total RNA was extracted (RNeasy mini system with Qiazol, Qiagen), treated with RNase-free DNase I (Roche) and re-purified using the RNeasy Minelute system (Qiagen). 0.25–1 μg of RNA was reverse-transcribed using Superscript-III (Life Technologies) according to the manufacturer's instructions. PCR was carried out using GoTaq (Promega). Sequences of individual primer pairs and PCR conditions are detailed in Supplementary Table S1. PCR products were visualized by agarose/ethidium bromide gel electrophoresis.

Immunocytochemistry

Cells were fixed for 20 min at room temperature in 4% paraformaldehyde (Fisher), with the exception of MSI1 staining where cells were fixed with ice cold 100% methanol for 20 min at −20 °C. Cells were blocked at room temperature in PBS/10% goat/2% BSA/Triton X-100 (0.1% for single cells or 0.3% for spheres). Primary antibodies were incubated overnight at 4 °C in PBS/2% goat serum/0.2% BSA/Triton X-100. Primary antibodies: OCT4 (SCBT, 1:50), SSEA-4 (DSHB, 1:4), NESTIN (Abcam, 1:300), MSI1 (Abcam, 1:200), SOX11 (Millipore, 1:5000), Ki67 (Vectorlabs, 1:300), TUJ1 (Abcam and Millipore, both 1:500), GFAP (Dako, 1:1000), GABA (Sigma, 1:500), TH (Millipore, 1:250), MAP2ab (Sigma, 1:250), ChAT (AB143, Millipore, 1:400), NKX2.1 (Abcam 1:100), Isl1 (Abcam, 1:500), and VAChT, (SySy 1:1000). Secondary antibodies were incubated at room temperature for 2 h in PBS/1% goat serum/Triton X-100. Cells were co-stained with Hoechst 33258 (Sigma) and mounted in Vectorshield (Vectorlabs). Staining was visualized using an upright fluorescent microscope. For TUJ1/GFAP and ChAT/TUJ1 cell counts a Leica SP5 confocal imaging system was used and image analysis carried out using Leica LAS confocal software. All images were processed using ImageJ and Adobe Photoshop CS3.

Taqman gene expression analysis of *LHX8*

Total RNA was extracted and processed as described. cDNA was generated using Taqman reverse transcription reagents, and the qPCR assay was carried out using the Taqman Universal Master Mix and Taqman assays for *LHX8* and *GAPDH* as the endogenous control (all Life Technologies). Each 20 μl reaction contained 100 ng cDNA.

SHH ELISA

Media was and stored at −80 °C. SHH in the media was assayed using a human specific ELISA kit (Abcam) according to the manufacturer's instructions. For comparison between differentiation protocols SHH was normalized against total protein in cell lysate.

Immunoblot

Cells were lysed in RIPA (50 mM Tris HCl pH 8, 150 mM NaCl, 1% NP-40, 0.5% sodium deoxycholate, 0.1% SDS) plus protease inhibitor (Roche). Protein was quantified using a BCA assay (Thermo Scientific) and 20 μg was resolved on a 12% polyacrylamide SDS-Tris-Glycine gel. Proteins were transferred onto a 0.45 μm PVDF membrane (Roche) which was blocked with 10% non-fat milk in TBS buffer with 0.1% Tween-20 (Sigma). Incubation with primary antibody (rabbit anti-p75 (Sigma) 1:1000; rabbit anti-NKX2.1 (Abcam) 1:1000, rabbit anti-Lhx8 (Genetex) 1:1000, rabbit anti-syn1 (SySy) 1:1000, and mouse anti-α-Tubulin (Sigma) 1:10,000) was carried out overnight at 4 °C in blocking buffer. Membranes were incubated with the appropriate HRP-labeled secondary antibody for 2 h at room temperature. Protein bands were visualized using Pierce Plus Substrate (Thermo).

Acetylcholine release assay

Acetylcholine release was assessed in 28-day terminally differentiated hPSC-derived neurospheres as described (Zoukhri and Kublin, 2002). We collected samples to assess both spontaneous and (Carbachol CCh; 50 μM) induced release using an Amplex Red Acetylcholine assay kit (Life Technologies).

Calcium imaging

Calcium imaging was carried out on 28-day terminally differentiated hPSC-derived neurospheres. Cells were washed with HBS buffer (mM: NaCl, 140; KCl, 3; Hepes, 10; glucose, 10; $CaCl_2$, 2; $MgCl_2$, 2; TTX, 500 nM; glycine, 1 mM; picrotoxin, 100 mM; pH 7.4; and osmolarity 300–310 mosmol l^{-1}) and loaded with 5 mM of the membrane-permeant Ca^{2+} indicator fluo-3 AM made up in 1 mg × ml^{-1} BSA/HBS at 37 °C for 25 min. Cells were washed and incubated for 20 min in natural atmosphere at 22 °C to allow de-esterification of the fluorophore. Cells were exposed to CCh (50 μM) and KCl (100 mM). Cells were viewed on a Leica DM IRBE fluorescence microscope, using a green filter set and perfused continuously with HBS buffer at ~2 ml × min^{-1}. One image was obtained every 5 s. Fluorescence of individual cells in each preparation was determined using Image J image analysis program (available at http://rsb.info.nih.gov/ij/) and expressed relative to baseline. The mean peak fluorescence was calculated.

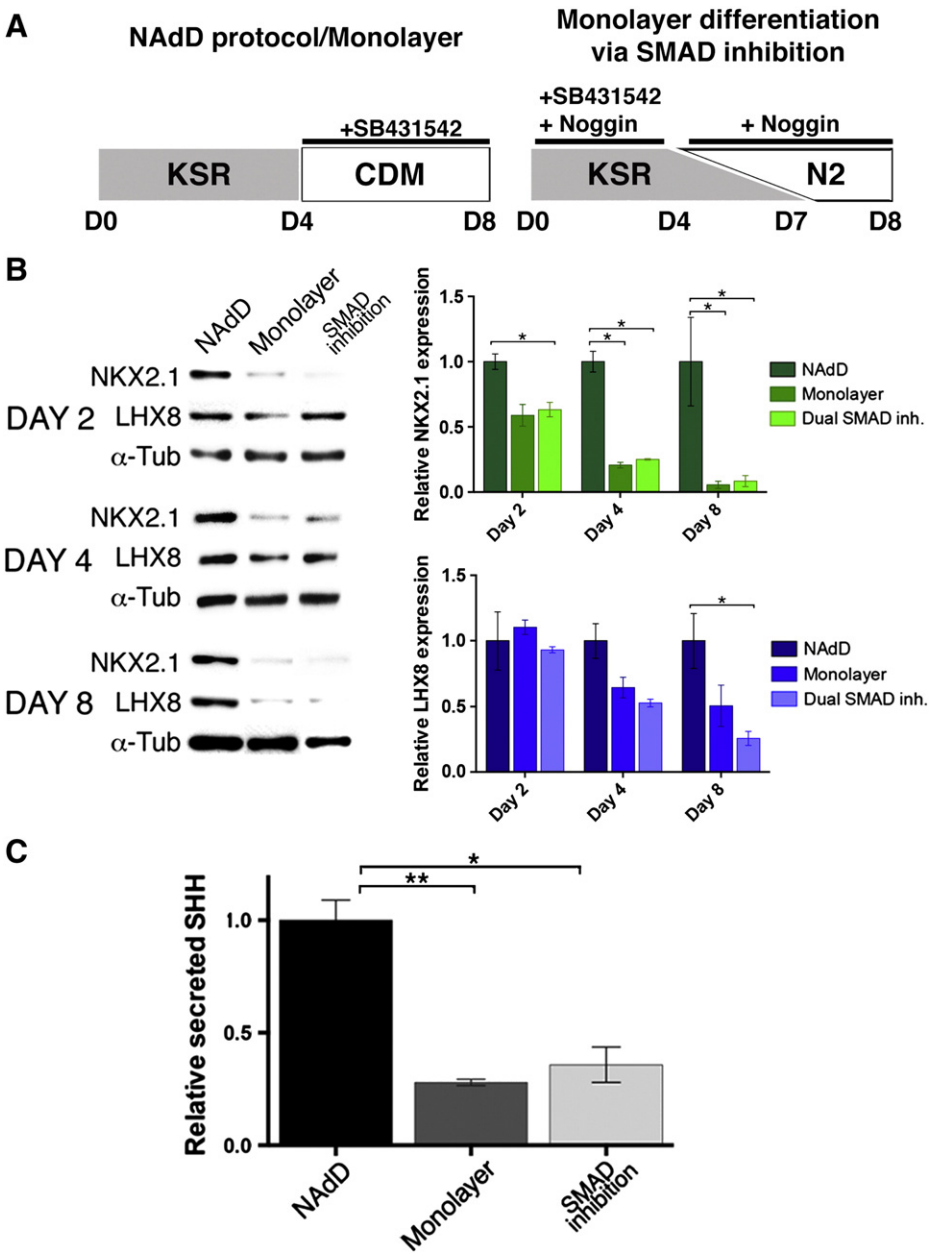

Figure 1 EB-based non-adherent differentiation (NAdD) demonstrated efficient induction of basal forebrain markers. (A) Schematic of the EB-based NAdD protocol, of which media components were also tested in a monolayer format, *versus* the monolayer dual SMAD inhibition protocol (Chambers et al., 2009). (B) Protein samples were collected on days 2, -4 and -8 of the three protocols, which we would consider the early inductive stage of the neural differentiation process. Immunoblot showed that expression of the basal forebrain marker NKX2.1 was highest in the NAdD system at all time points examined, compared to monolayer differentiation of hPSCs either in the same media components as were used in NAdD), or *via* dual SMAD inhibition which is an established monolayer method of hPSC differentiation (Chambers et al., 2009) (days 2 and 4 n = 2, day 8 n = 5 SEM, two tailed *t*-test). By day 8, Lhx8 expression was higher in the NAdD protocol compared to the other two protocols. (C) The mature hedgehog ligand, SHH was present at significantly higher levels in the NAdD protocol after 4 days of differentiation, compared to monolayer differentiation of in either the same media components as were used in NAdD (n = 2, SEM, two tailed *t*-test; ** p = <0.05), or *via* dual SMAD inhibition (Chambers et al., 2009) (n = 2, SEM, two tailed *t*-test; * p = <0.05). For comparison between differentiation protocols SHH was normalized against total protein in cell lysate.

Electrophysiology

For electrophysiology, after 28 days NEM media was replaced with modified neuronal differentiation media (NDM) (Johnson et al., 2007) containing 1 μg/ml laminin and 0.1% horse serum (Life Technologies) and cells were allowed to differentiate for a subsequent 5–6 weeks. For whole-cell recordings, coverslips were transferred to the recording chamber, and submerged in aCSF, (mM: 124 NaCl, 3 KCl, 26 $NaHCO_3$, 1.25 NaH_2PO_4, 2 $CaCl_2$, 1 $MgSO_4$ and 10

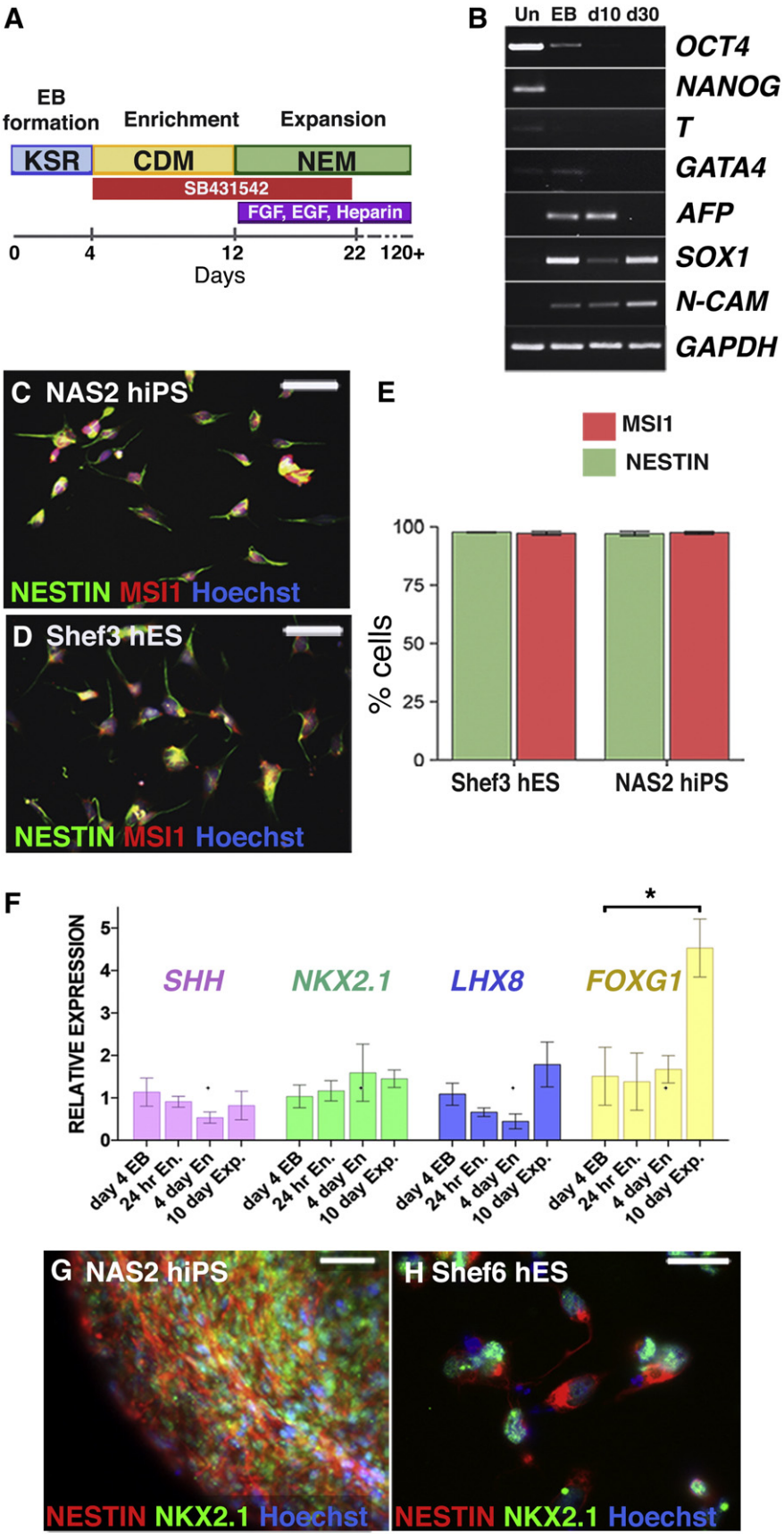
A
EB formation
Enrichment
Expansion
KSR
CDM
NEM
SB431542
FGF, EGF, Heparin
0
4
12
22
120+
Days
B
Un EB d10 d30
OCT4
NANOG
T
GATA4
AFP
SOX1
N-CAM
GAPDH
C NAS2 hiPS
NESTIN MSI1 Hoechst
D Shef3 hES
NESTIN MSI1 Hoechst
E
MSI1
NESTIN
% cells
100
75
50
25
0
Shef3 hES
NAS2 hiPS
F
RELATIVE EXPRESSION
SHH
NKX2.1
LHX8
FOXG1
*
day 4 EB
24 hr En.
4 day En
10 day Exp.
G NAS2 hiPS
NESTIN NKX2.1 Hoechst
H Shef6 hES
NESTIN NKX2.1 Hoechst

D-glucose, bubbled with 95% O_2/5% CO_2). Intracellular pipette (4–6 MΩ) solutions comprised (mM): 140 K-gluconate, 10 HEPES, 10 BAPTA, and 4 Mg^{2+}-ATP, pH 7.2, 290 mOsm. For recording spontaneous activity, the pipette solution contained (mM): 20 KCl, 121 K-gluconate, 10 HEPES, 10 BAPTA, and 4 Mg^{2+}-ATP, pH 7.2, 290 mOsm. Cells were voltage-clamped at a resting membrane potential between −60 mV and −70 mV. During current-clamp recordings, 40 pA current injection was maintained. Clamp recordings were carried out using an Axopatch 700B amplifier (Axon Instruments). Current signals were captured on-line by a 486 computer at a sampling frequency of 2 kHz, and digitized at 10 kHz with the voltage signal *via* a 1200 Digidata interface digitizer (Axon Instruments). Only cells with series resistance of <25 MΩ with a change in series resistance of <10% from the start were included in this study. The frequency of spontaneous activity was measured for each experiment and normalized as mean values ± sem. Background noise threshold was set at 10 pA to determine spontaneous responses, therefore spikes larger than 20 pA were included in frequency calculations. Acquired data was analyzed using OriginPro 7.5. All experiments were performed at 27–29 °C. TTX (500 nM, Sigma) was used where indicated.

Transplants

10-week old, female Lewis rats (Harlan, UK) received a unilateral graft to the medial septum (MS; n = 6. AP, +0.7; ML, +0.2; DV, −7.0) (Wu et al., 2002). 3 days prior to surgery hPSC-derived neurospheres were chopped at 200 μm and media was supplemented with laminin (1 μg/ml). 10-small neurospheres, (~35,000 cells) were loaded in 5 μl NEM into a 5 μl zero-dead volume, plunger-in-the-needle SGE glass micro-syringe incorporating a 30-gauge stainless steel blunt cannula (Fisher Scientific, UK). Rats were immunosuppressed with a daily subcutaneous injection of Cyclosporin A (10 mg/kg, Sandimmune, Sandoz), which began 48 h prior to surgery and continued thereafter. Grafts were analyzed 8–9 weeks post surgery.

Immunohistochemistry

Animals were terminally anesthetized and transcardially perfused with 4% paraformaldehyde. Brains were post-fixed overnight and dehydrated in 30% sucrose in 0.1 M phosphate buffer. 40 μm free-floating sections (1 in 6 series) were blocked for 2 h in PBS/20% goat serum/2% BSA/0.1% Triton X-100. Primary antibodies were incubated overnight at 4 °C in PBS/2% goat serum/0.2% BSA/0.1% Triton X-100, followed by a 2 h incubation in secondary antibodies made up in 2% PBS/2% goat serum/0.2% BSA/0.1% Triton X-100. Primary antibodies used were mouse anti-HNA (1:400, Millipore), rabbit anti ChAT (1:400, Millipore) and rabbit anti-Double Cortin (DCX; Abcam; 1:500).

Results

Induction of ventral forebrain markers in hPSCs by embryoid body *versus* adherent differentiation methods

The most evident way to manipulate hPSC differentiation in the absence of extrinsic factors was to manipulate the physical environment to which the differentiating hPSCs were exposed. Therefore we compared three methods for the neural induction; EB-based NAdD *versus* differentiation as a monolayer, with the comparison essentially being between a 3D environment, more similar to that in the early embryo, *versus* an adherent, 2D environment respectively. EB formation recapitulates the early embryonic environment to provide cues for acquisition of cell fate. This results in differentiation of the three embryonic germ layers mesoderm, endoderm and ectoderm, the latter giving rise to the neuroectoderm and thus NSCs (Fig. 1A) (Martin and Evans, 1975).

We generated EBs from aggregates of hPSCs in Knock-out Serum Replacer (KSR) based media, in the presence of ROCK inhibitor, Y-27632, both of which promote cell survival (Fig. 1A) (Watanabe et al., 2005) (Watanabe et al., 2007). After 4 days EBs were transferred into a chemically defined media (CDM), containing the Nodal/TGF-β inhibitor, SB431452, to promote differentiation and expansion exclusively of neural cells, rather than mesendodermal fates (Fig. 1A) (Joannides et al., 2007; Chambers et al., 2009; Vallier et al., 2004). In parallel hPSCs were differentiated as a monolayer in the same media components as the NAdD protocol. We also employed a third technique, a widely used monolayer based method, developed by Chambers et al. (2009), termed dual SMAD inhibition (Fig. 1A). This protocol differentiates hPSCs as a monolayer in

Figure 2 The optimized NAdD protocol could efficiently and reproducibly generate NSCs with a basal forebrain phenotype. (A) Schematic of the differentiation protocol used for neural induction of the hES lines, Shef2, Shef3 and Shef6, and the hiPS lines NAS2 and MSUH0001. (B) RT-PCR demonstrated that differentiating hPSCs showed rapid down-regulation of pluripotency markers (*OCT4*, *NANOG*), unregulation of mesendoderm markers (*T*, *GATA4*, *AFP*) and neuroectoderm markers (*SOX1*, *N-CAM*). Neural enrichment and expansion resulted in exclusive neural marker expression (*SOX1*, *N-CAM*), indicating a pure population of NSCs. *GAPDH* was the endogenous control. (C–*E*) Immunocytochemistry on acutely plated 30-day expanded single NSCs demonstrated equivalently high numbers of $NESTIN^+/MSI1^+$ cells from the hiPS (C) and hES lines (D) as confirmed by quantification of cell numbers (E >97%, n = 3, n = 2 respectively, SEM, $P > 0.05$). (F) Quantitative PCR demonstrated expression profiles of genes involved in ventral forebrain development over the duration of the NAdD protocol. For ventral specific markers we saw relatively consistent expression, showing no statistically significant changes, however we saw a significant increase in the general forebrain transcription factor *FOXG1* which increased when hPSC-derived NSCs were in the expansion stage of the protocol (n = 4). (G, H) The basal forebrain phenotype was confirmed by immunocytochemistry showing $NKX2.1^+/NESTIN^+$ NSCs within the expanding NAS2 hiPS-derived neurosphere (G), and also upon acute plate-down of Shef6 hES derivatives (H). Scale bars: (C, D) 50 μm; (G) 100 μm; (H) 25 μm.

the presence of SB431452 and Noggin, an inhibitor of SMADs downstream of BMP signaling, which promotes neural differentiation (Fig. 1A). At days 2, 4 and 8, samples were taken from the three protocols and screened by immunoblot for the basal forebrain transcription factors NKX2.1 and LHX8 (Nat and Dechant, 2011; Liu, 2011) (Fig. 1B). At all time points examined NKX2.1 was expressed at higher levels in cells undergoing neural differentiation in the NAdD protocol, compared to either of the monolayer differentiation protocols (Fig. 1B). LHX8 was expressed at similar levels at the start of differentiation across the protocols, but by day 8 expression of LHX8 was higher in the NAdD protocol *versus* either of the monolayer protocols (Fig. 1B). From this experiment we concluded that the EB-based NAdD protocol generates a basal forebrain identity during neural differentiation with greater efficiency than neural differentiation of hPSCs as a monolayer.

In the developing embryo acquisition of basal forebrain identity is regulated by hedgehog signaling, with secretion of the SHH ligand from tissues adjacent to the ventral neural tube, and then the ventral neural tube itself (Ericson et al., 1995a; Echelard et al., 1993; Ericson et al., 1995b; Shimamura and Rubenstein, 1997). Therefore we hypothesized that the high levels of NKX2.1 and LHX8 expression seen in the NAdD protocol must be due to higher levels of secretion of the mature form of the hedgehog ligand, SHH, compared to the two monolayer protocols. An ELISA on media collected from day 4 of each protocol confirmed 2–3 fold higher amounts of SHH secretion in the NAdD protocol compared to the monolayer protocols (Fig. 1C). Together this data clearly demonstrated that regardless of basic media composition, the physical environment in which the cells differentiated ultimately determined their acquisition of a basal forebrain fate, and this was due to the positive influence of the non-adherent 3D differentiation environment on hedgehog signaling.

Efficient NAdD of hES and hiPS cells into an expanding population of NSCs

We went on to optimize the NAdD protocol with the aim to produce a pure population of basal forebrain-like NSCs. We extended the period of neural enrichment in CDM, after which cell aggregates were transferred into Neural Expansion Media (NEM) containing the growth supplement B27 plus FGF2, EGF and heparin and expanded as non-adherent neurospheres, similar to their human fetal counterparts (Anderson et al., 2007; Svendsen et al., 1998; Carpenter et al., 1999; Vescovi et al., 1999). The optimized protocol therefore consisted of three specific stages; 1) EB formation, 2) neural enrichment, and 3) expansion as non-adherent neurospheres (Fig. 2A, Supplementary Fig. S1A). RT-PCR demonstrated rapid down-regulation of pluripotency markers and expression of various germ layer markers (Fig. 2B). We found extending the enrichment period to 8 days, in addition to maintenance of SB431452 throughout enrichment and the first 10 days of expansion was required to achieve a pure population of expanding NSCs, as indicated by RT-PCR at day 30 of expansion (Fig. 2B).

This was confirmed by the high percentages of single plated cells that co-expressed the NSC markers NESTIN and MSI1 (Figs. 2C, D). We saw no difference in the efficiency of neural conversion of hES compared to hiPS lines, of which over 97% were positive for each marker (Fig. 2E). Furthermore similar results were achieved with every hPSC line differentiated *via* NAdD (Figs. 2C–E, Supplementary Figs. S1B–E).

To evaluate at what stage of the NAdD protocol the ventral telencephalic identity was induced we profiled the expression of a number of genes involved in early regionalization of the telencephalon. These were the ventral telencephalic markers, *SHH*, *NKX2.1* and *LHX8*, in addition to the general forebrain transcription factor *FOXG1* (Fig. 2F). Expression of the ventral marker genes *SHH*, *NKX2.1* and *LHX8* was present from EB stage of the protocol (day 4) and there were no significant changes in their expression levels for the duration of the NAdD protocol (Fig. 2F). This confirmed that ventral identity of the cells was induced from the earliest EB stage of the protocol. This would agree with the expression of SHH in the media at this stage, as shown in Fig. 1C. We did however see a 3-fold increase in the expression of *FOXG1* 10 days into the expansion stage of the protocol (Fig. 2F). This could be due to the presence of FGF2 in the expansion media. FGF signaling directly induces FOXG1 expression in the developing telencephalon, and this specifically involves the FGFRs to which FGF2 is known to bind (Shimamura and Rubenstein, 1997).

We confirmed continual expression of the NKX2.1 protein by immunoblot (Supplementary Fig. S1F), and immunocytochemistry demonstrated NKX2.1 expression in the expanding hPSC-derived neurospheres and also acutely plated NSCs (Figs. 2G, H). We quantified the proportion of NKX2.1 expressing cells within the population and found that for the NAS2 hiPS-derived NSCs, 92.87 ± 3.22% of the NESTIN expressing also expressed NKX2.1 (n = 2, SEM). This confirmed that the NAdD protocol efficiently and reproducibly induces a basal forebrain phenotype.

We next assessed NSC marker expression after 90 days expansion, considered a 'long-term' culture period. *DACH1* and *PLAGL1*, which are considered markers of the earliest definable NSC were expressed and maintained (Fig. 3A) (Elkabetz et al., 2008). NESTIN and MSI1 were present in the same high proportion of cells (Fig. 3B). Expression of the definitive NSC marker SOX1 was also maintenance in 90-day expanded hiPS and hES-NSC populations (Figs. 3C, D). Importantly we saw maintained expression of NKX2.1 after 90 days expansion (Figs. 3E, F). Together these findings suggested the 'stemness' of the NSCs and their basal forebrain identity was maintained, even with long-term expansion in culture.

Confirmation that hedgehog signaling the EB is responsible for ventralization of the hPSC-derived NSCs

It is well established that in the developing basal forebrain hedgehog signaling is responsible for early induction of ventral identity in neural progenitors, resulting in the expression of NKX2.1 and *LHX8* (Nat and Dechant, 2011; Liu, 2011). Further analysis of secreted SHH levels in the EB media showed a significant decrease between day 2 and day 4 suggesting that secretion of SHH was highest in the earliest stages of germ layer differentiation (Fig. 4A). This was therefore prior to the

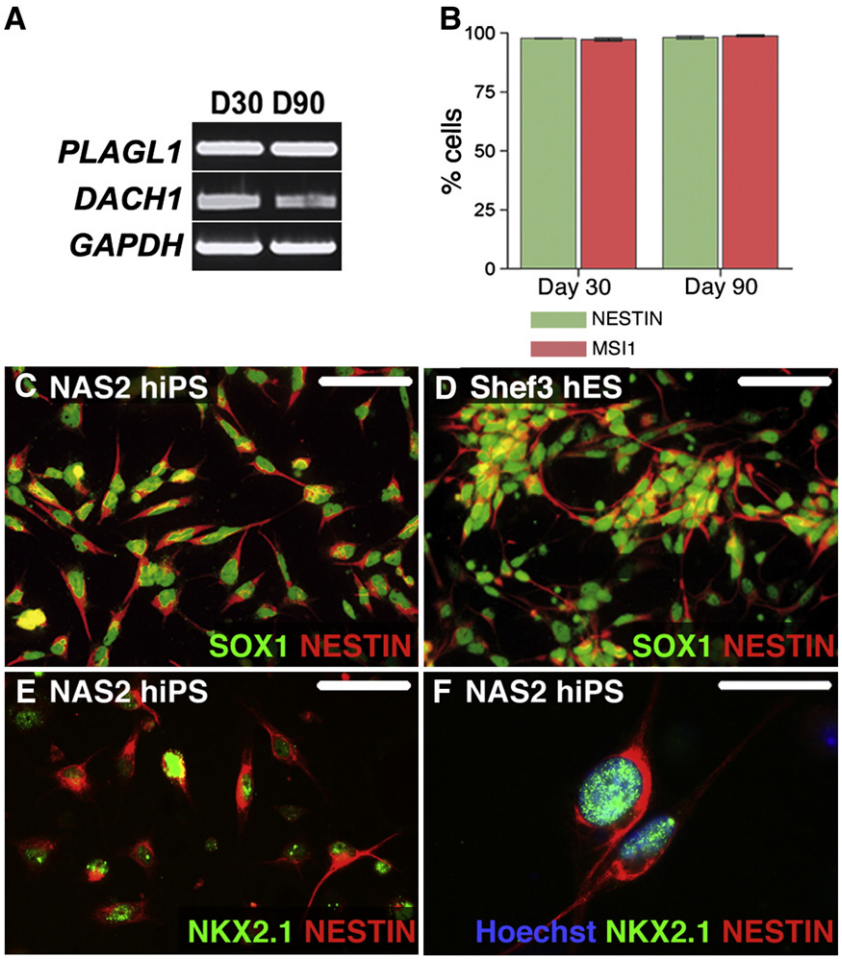

Figure 3 The basal forebrain progenitor phenotype of the hPSC-derived NSCs was maintained throughout expansion in culture. (A) Semi-quantitative RT-PCR revealed that the hPSC-derived NSCs demonstrated expression of early neural 'rosette' markers *DACH1* and *PLAGL1* after 30 days in expansion (D30), and this was maintained at the later time-point, after 90 days. (B) Similarly, immunocytochemistry and subsequent quantification of the Shef3 hES-derived NSCs revealed maintenance of the stem cell markers NESTIN and MSI1 from 30 to 90 days in culture. This suggested that by generating hPSC-derived NSCs *via* NAdD produced an NSC population, which retained the same phenotype even after multiple proliferations and passages (>98% n = 3, SEM). (C, D) Further confirmation came from immunocytochemistry demonstrating continued expression of the definitive NSC marker, SOX1, shown here alongside NESTIN, after a 90 day expansion period of both the NAS2 hiPS and Shef3 hES-derived NSCs. This also established that maintenance of a neural progenitor phenotype was universal, regardless of the hPSC line. (E, F) Critically hPSC-derived NSCs also maintained their basal forebrain characteristics throughout expansion, as demonstrated by their continued expression of NKX2.1 at 90 days in culture, shown here alongside NESTIN. Scale bars: (C, D, E) 50 μm; (F) 25 μm.

addition of the Nodal inhibitor SB431542, or the morphogens FGF2 and EGF and in the absence of any factors known to influence dorso-ventral patterning, or hedgehog signaling. This therefore confirmed that it was the environment of the EB that led to the initiation of hedgehog signaling *via* secretion of SHH.

For further validation that SHH was responsible for the observed basal forebrain phenotype we exposed EBs to cyclopamine, a potent inhibitor of downstream hedgehog-signal transduction. We used NKX2.1 protein levels as a read-out for active hedgehog signaling, as NKX2.1 expression is positively regulated by SHH (Ericson et al., 1995a; Pera and Kessel, 1997). EBs were exposed to cyclopamine (50 μM) for the first 4 days of the neural enrichment in CDM and we saw a robust reduction in levels of NKX2.1 (Fig. 4B).

We went on to further establish the extent to which this protocol recapitulated the development of bfCNs *in vivo*. Accurate reproduction of embryonic fate acquisition would be critical should these cells be used as a model to study bfCN neurogenesis *in vitro*. $NKX2.1^+/NESTIN^+$ NSCs present 12 h after mitogen withdrawal (Fig. 4C) start to terminally differentiate into $NKX2.1^+/TUJ1^+$ neuronal progenitors by 24 h (Figs. 4D, E). Finally the mature hPSC-derived bfCNs also expressed ISL1, a transcription factor, present in mature cholinergic neurons (Fig. 4F) (Elshatory and Gan, 2008). These findings confirmed intrinsic hedgehog signaling in the EB formation stage, thus that NAdD induces a ventral telencephalic phenotype, which mimics that of differentiating bfCNs within the MGE of the embryonic telencephalon.

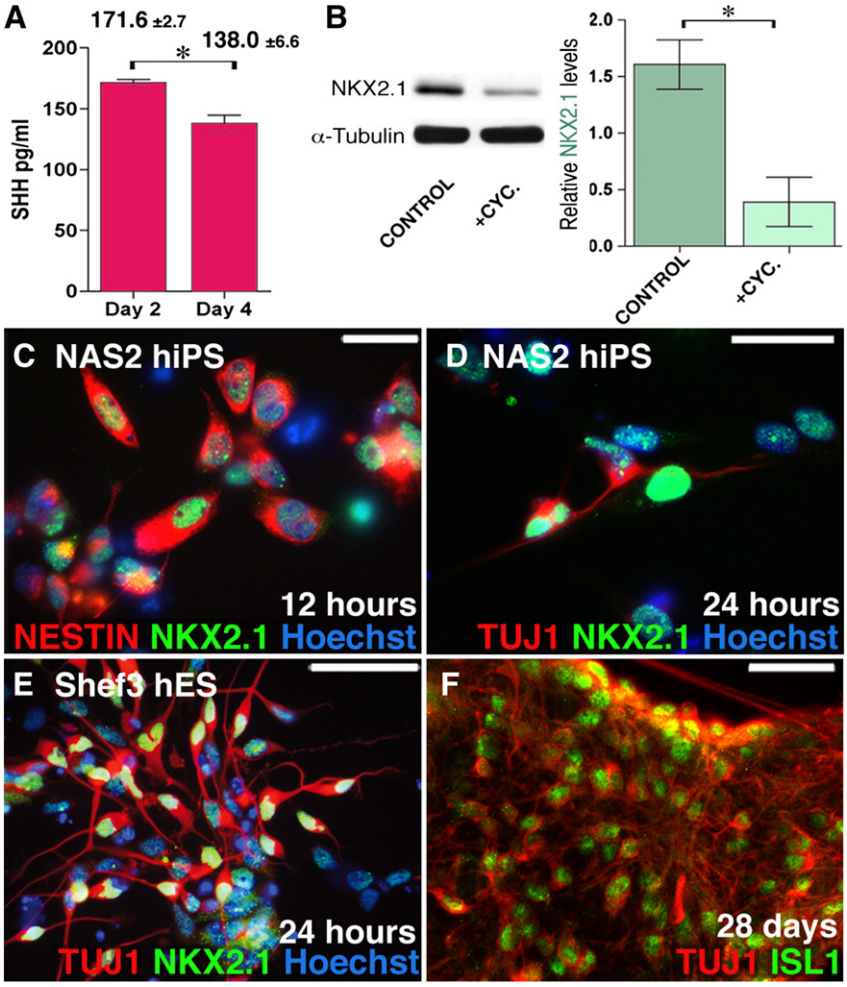

Figure 4 Hedgehog signaling is responsible for the ventralization of the hPSC-derived NSCs, which recapitulate *in vivo* differentiation of bfCNs in the basal forebrain upon mitogen withdrawal. (A) Secreted SHH was detected in day 2 and day 4 EB media (n = 2, SEM, two tailed *t*-test * p = <0.05). (B) Addition of the hedgehog antagonist cyclopamine for 4days as EBs entered neural enrichment resulted in a significant reduction in NKX2.1 protein levels (n = 3, SEM, two tailed *t*-test *P = <0.05). This therefore confirms that intrinsic hedgehog signaling in the NAdD system is responsible and sufficient to ventralize the cells, resulting in evident basal forebrain characteristics. (C–*E*) NKX2.1 was co-expressed with NESTIN by the hPSC-derived NSCs 12h after mitogen withdrawal (C), and maintained in TUJ1$^+$ neuronal progenitors 24 h after mitogen withdrawal (D,E). (F) Terminally differentiated hPSC-derived TUJ1$^+$ neurons also co-expressed basal forebrain, cholinergic transcription factor, ISL1. This hedgehog regulated temporal expression of NKX2.1, followed by expression of ISL1 marks the transition from basal forebrain progenitor to bfCN, as occurs in the developing embryonic brain. Scale bars: (C, D) 25 μm; (D, E) 50 μm.

NAdD derived NSCs generate high numbers of cholinergic neurons

After terminal differentiation, immunocytochemistry analysis of the hPSC derivatives revealed the presence of both class III β-Tubulin (TUJ1)$^+$ neurons and GFAP$^+$ glial cells (Figs. 5A–D). Quantification using confocal microscopy throughout and surrounding the terminally differentiated neurospheres revealed a high percentage of neurons (87.82% ±2.04, SEM, n = 3, Fig. 5E).

We went on to further characterize the subtype of the neurons generated in this study. Widespread expression of the ventral cholinergic transcription factor ISL1, as shown in Fig. 4F, was evidence that a cholinergic neuronal subtype was generated from the hPSC-derived NKX2.1$^+$ NSCs. Further immunocytochemistry analysis confirmed that the majority of neurons in the population were cholinergic, co-expressing TUJ1 with Choline AcetylTransferase (ChAT) (Fig. 5F). Quantification using confocal microscopy throughout and surrounding the terminally differentiated neurospheres revealed 90.9 ± 1.54% of the Shef3 hES-derived neurons (SEM, n = 3) and 92.39 ± 2.31% of the NAS2 hiPS-derived neurons (SEM, n = 2) were in fact cholinergic (Fig. 5G). TUJ1$^+$/ChAT$^+$ neurons were present throughout the center of the terminally differentiated neurospheres, where ChAT was distributed in the cytoplasm (Fig. 5H). We also saw TUJ1$^+$/ChAT$^+$ neurons in the area

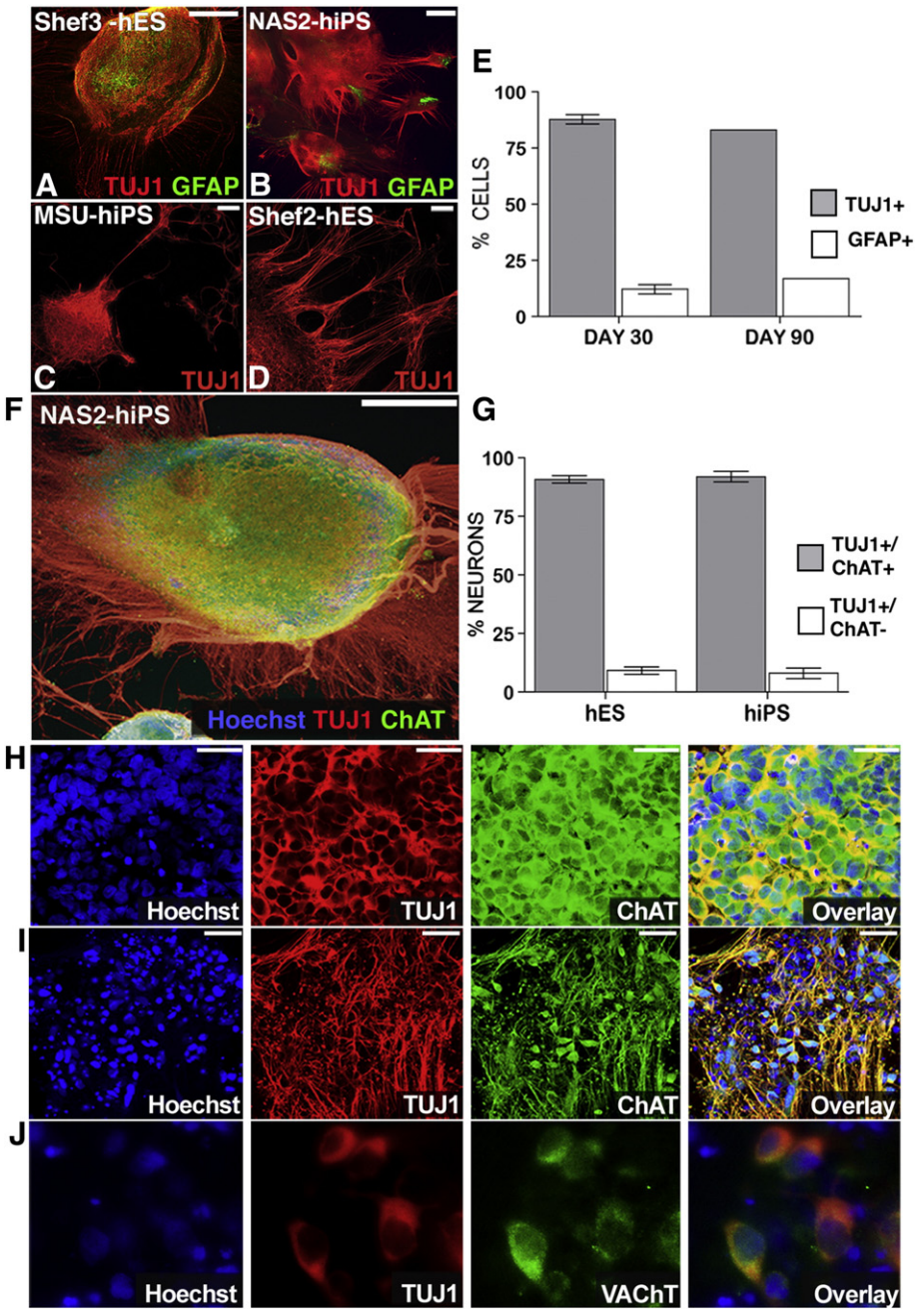

Figure 5 hPSC-derived NSCs demonstrate a propensity towards cholinergic neuronal differentiation. (A) 28-day terminally differentiated Shef3 hES-derived neurospheres predominantly consisted of TUJ1$^+$ neurons, intermixed with GFAP$^+$ glial progeny. (B–D) This high neurogenic capacity was consistently demonstrated by each hPSC line differentiated using the NAdD system, as shown by the high numbers of TUJ1$^+$ neurons. (E) Quantification of Shef3 hES derivatives by confocal microscopy confirmed this propensity towards neuronal differentiation, with hES-derived NSCs generating 87.82% neurons upon terminal differentiation (n = 3, SEM). After a 90-day expansion period of expansion in culture, the hES-derived NSCs maintained this neurogenic capacity, with 83.06% being TUJ1$^+$ neurons (n = 2, SEM). (*F*) Further characterization revealed that the majority of neurons were cholinergic, Co-expressing TUJ1, and the cholinergic marker ChAT. (G) Quantification revealed 90.9% of the Shef6 hES-derived neurons and 92.39% of the NAS2 hiPS-derived neurons were ChAT$^+$ (n = 3, n = 2 respectively, SEM), confirming that the NAdD system of differentiation produced a basal forebrain, cholinergic phenotype, regardless of the identity of the parent cell line. (H, I) Detailed confocal microscopy was used for quantification of cell numbers, revealing ChAT$^+$/TUJ1$^+$ neurons throughout the center (*H*) and also around the edge of the neurosphere (I). (J) The terminally differentiated neurons were also VAChT$^+$, another marker of cholinergic neurons shown here with the neuronal marker MAP2ab. Scale bars: (A, B, F) 250 μm; (H) 25 μm; (C, D, I and J) 50 μm.

surrounding the neurosphere (Fig. 5I). Further verification of the cholinergic phenotype was provided by expression of the Vesicular Acetylcholine Transporter (VAChT), the protein responsible for loading acetylcholine into synaptic vesicles, another specific marker of cholinergic neurons (Fig. 5J). Within the differentiated neurospheres we also saw small numbers of GABAergic neurons and Tyrosine Hydroxylase (TH) expressing dopaminergic neurons, which are two neuronal subtypes also found in the forebrain (Supplementary Figs. S2 A and B).

Together this data demonstrated that the NAdD system of differentiation of hPSCs, *via* an expandable basal forebrain-like NSC, was able to reproducibly and preferentially generate high numbers of neurons, of which the majority, over 90% on average, were cholinergic.

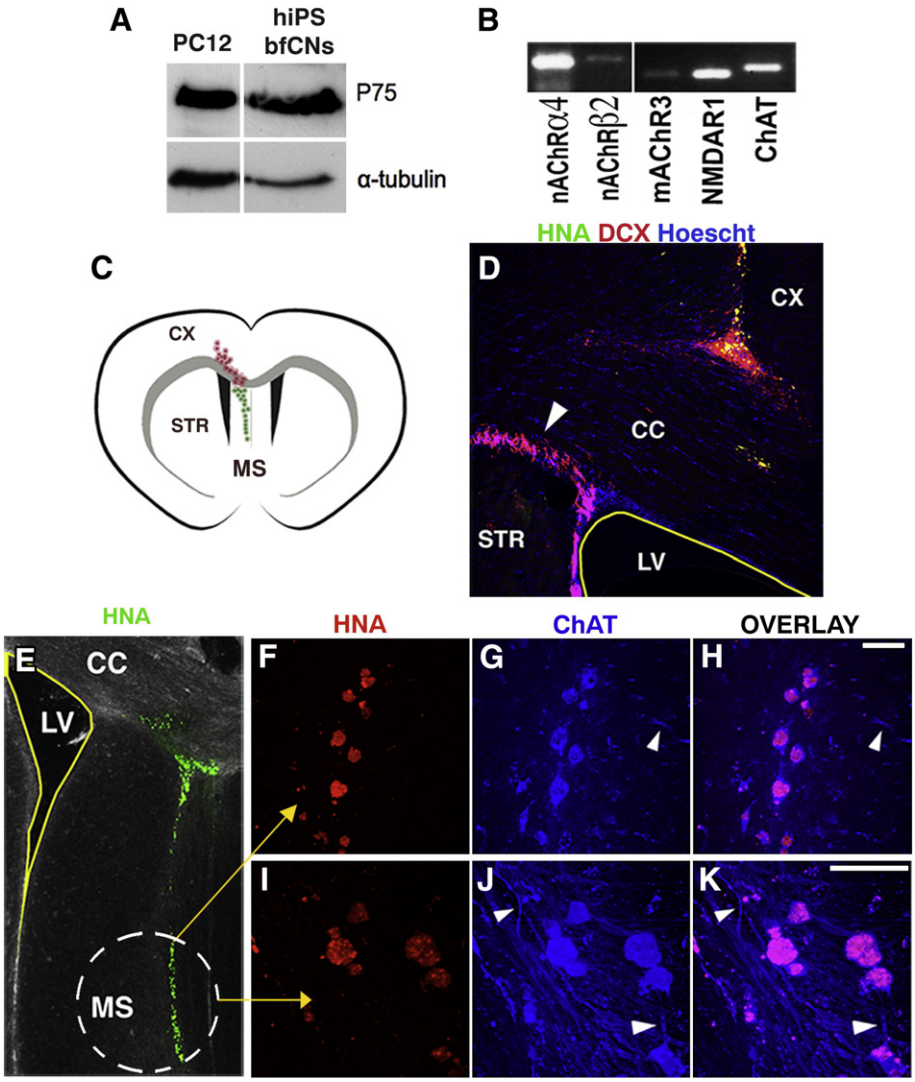

Figure 6 The hPSC-derived bfCNs possessed a phenotype characteristic of those in the adult brain. (A) NAS2 hiPS-derived neurons expressed of $p75^{NTR}$ at high levels, comparable to that of PC12 cells (Masoudi et al., 2009). (B) RT-PCR demonstrated expression of the cholinergic receptor subunit genes *nAChR4*, *nAChRb2* and *mAChR3*, in addition to the glutamate receptor gene *NMDAR1*. *ChAT* was used as an endogenous control for the presence of cholinergic neurons. (C) hES and hiPS-derived NSCs were grafted into the MS of adult rats. As shown in this schematic of the rat forebrain HNA^+ human grafted cells were found in two specific areas, within the overlying CX (red dots), and also in MS (green dots). (D) As shown here in a Shef6 hES-derived NSC graft, HNA^+ cells only expressed the immature neuronal marker, DCX, when present in the CX. Interestingly HNA^+/DCX^+ cells were never present within the underlying MS. The white arrowhead indicates the endogenous DCX^+ progenitors within the ventricular zone of the rat's lateral ventricle. (E–K) Within the MS the grafted HNA^+ cells spanned the majority of the dorso-ventral range of the MS, but $ChAT^+$ cells were only found in the more ventral region, as indicated by the dashed line on (E). High magnification confocal z-stacks were used to image the HNA^+ cells co-expressing ChAT within the MS (F–K). The cells within the graft were closely associated with ChAT positive projections (filled arrow heads). HNA, human nuclear antigen; CX, cortex; MS, medial septum; CC, corpus collosum; LV, lateral ventricle; STR, striatum; DCX, doublecortin. Scale bars: (F–L) 40 μm.

NAdD generates bfCNs with a phenotype typical of a human adult bfCN

We further characterized the neurons to establish their suitability as a model of bfCNs in the mature human brain. In the adult brain the neurotrophin receptor $p75^{NTR}$ is expressed by over 90% of bfCNs and is a key mediator in cholinergic signaling and hippocampal innervations from the basal forebrain (Allen and Dawbarn, 2006; Coulson et al., 2009). Crucially immunoblot analysis established high levels of the $p75^{NTR}$ protein in hiPS-NAS2-derived neurons (Fig. 6A). Furthermore, RT-PCR demonstrated expression of various important receptor subunit genes (*nAChRa4* and *nAChRb2*, *mAChR3*, *NMDAR1*), which while not specific to bfCNs, are required for the correct function of these neurons within the basal forebrain (Fig. 6B) (Whiting and Lindstrom, 1988; Griguoli and Cherubini, 2012).

If the hPSC-derived NSCs were phenotypically similar to basal forebrain progenitors we would predict that they would be able to survive and integrate into the basal forebrain *in vivo* (Wu et al., 2002). 10 small hES- or hiPS-derived neurospheres were injected into the medial septum of 6 adult rats and the grafts were analyzed 8–9 weeks post surgery. Immunohistochemistry for Human Nuclear Antigen (HNA) allowed us to distinguish human cells, revealing three main areas where cells had integrated into the forebrain; the medial septum (MS), the overlying white matter of the corpus collosum (CC) and the cortex (CX) (Fig. 6C). We found that HNA positive cells within the CX co-expressed the immature neuronal marker Doublecortin (DCX) (Fig. 6D). HNA^+ cells within the MS expressed ChAT, indicating cholinergic neurons within the grafts (Figs. 6E–K and Supplementary movie 1). Interestingly DCX was absent from the MS grafts suggesting the $HNA^+/ChAT^+$ neurons were more mature than those cells found in the cortex. Importantly there was no evidence of teratoma formation. This *in vivo* survival is a major step forward in the application of hPSCs in the study of AD confirming the potential for cell replacement therapy. This also augments the other findings we present herein that phenotypically accurate human bfCN can be generated from hPSCs, which is of a standard to use as a model of the adult basal forebrain cholinergic system.

hPSC-derived NSCs generate neurons that demonstrate mature electrophysiological properties

Calcium imaging was used to assess the gross physiological activity of neurons within the total population. We stimulated the hPSC-derived bfCNs with both KCl to induce a membrane potential, and the cholinergic agonist Carbachol (CCh). We found a robust and widespread response to both, as shown by the single cell traces in Fig. 7A. These neurons demonstrated a robust and consistent response, with CCh inducing a 47.5% ± 7.9 increase and KCl producing a 67.3% ± 8.1 increase in fluorescence above baseline (98 cells were examined in total from 6 independent coverslips, SEM) (Fig. 7B). This indicated that the hPSC-derived bfCNs possessed both functional voltage-gated channels, and functional cholinergic receptors, which were also able to induce channel opening. In total 84.7% of KCl responding neurons were also responsive to CCh, therefore confirming the primarily cholinergic phenotype within these cultures. Further confirmation of their functionality came with our finding that the hPSC-derived bfCNs could release ACh, both spontaneously, and at an increased rate in response to the cholinergic agonist CCh (Fig. 7C).

Ultimately a neurons function is its ability to communicate electrically *via* its synapses. We therefore used whole-cell patch clamp recording to analyze neuronal action potential and spontaneous excitatory postsynaptic currents to assess the electrophysiological properties of the hPSC-derived bfCNs. The injection of current elicited an action potential, which was reversibly blocked by the selective sodium channel blocker, tetrodotoxin TTX (n = 5, Fig. 7D). We also saw robust spontaneous firing activity, which was also completely blocked by TTX, but recovered after removal of TTX (n = 6, Figs. 7E, F). These findings demonstrate the successful generation of functionally active neurons, therefore suggesting they are applicable as a functional *in vitro* model. Furthermore we carried out an immunoblot on protein extracted from cultures equivalent to those used for the electrophysiology and demonstrated expression of the synaptic marker Synapsin1. This suggests that the hPSC-derived bfCNs are forming synapses, which is key to their function (Fig. 7G).

Discussion

We have demonstrated the efficient generation of high numbers of bfCNs from hPSCs *via* an expandable basal forebrain NSC intermediate. This is of particular interest as bfCNs are one of the primary populations affected in AD, and our protocol provides a robust resource for their *in vitro* study (Holtzman et al., 2011; Everitt and Robbins, 1997; Davies and Maloney, 1976). This work is highly relevant in light of the recent advent of iPS technology, which has opened up the possibility of modeling diseases from a patient's own tissue (Han et al., 2011).

In the embryo the basal forebrain develops from the most ventral part of the embryonic telencephalon, and this ventral identity is induced by hedgehog signaling, *via* the SHH ligand (Fig. 8) (Ericson et al., 1995a; Shimamura et al., 1995; Pera and Kessel, 1997; Gunhaga et al., 2000). Regardless of the original cell line we could reproducibly and efficiently generate NSCs with a basal forebrain phenotype using EB-based, non-adherent differentiation or NAdD (Fig. 8). Specifically we have shown that NAdD generates higher levels of secreted SHH compared to differentiation as a monolayer, and this is true regardless of media composition. Furthermore, hedgehog signaling is initiated at the stage of early germ layer differentiation in the EB, the first stage of the NAdD protocol, and prior to the addition of any exogenous factors or morphogens, which could influence dorso-ventral cell fate. Timing of this ventral patterning is in agreement with events in the developing embryo where the hedgehog signaling is induced relatively early in development as the germ layers develop adjacent to the ventral neural tube (Fig. 8) (Briscoe and Ericson, 1999). Therefore we conclude that it is the unique 3D environment of the EB, which is sufficient to recapitulate these developmental events *in vitro*.

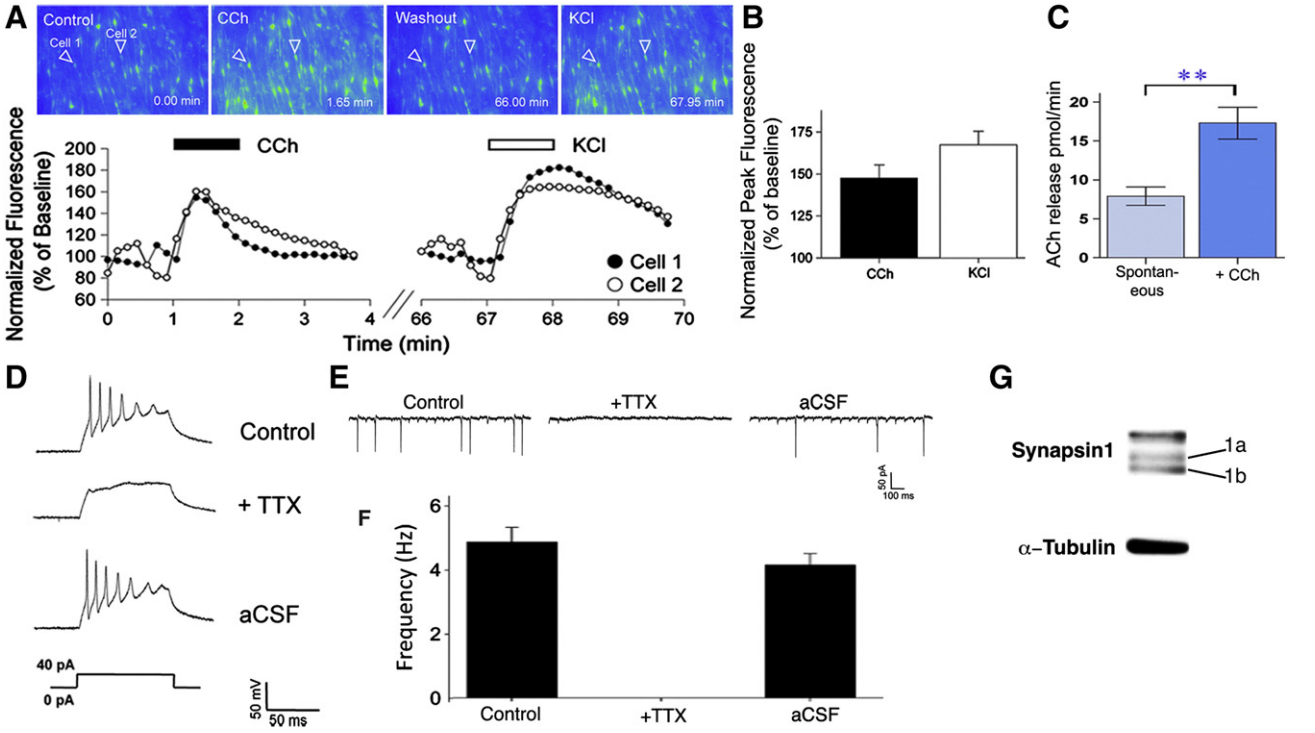

Figure 7 hPSC-derived neurons demonstrated physiological and electrical properties typical of mature, functional neurons. (A) Calcium imaging demonstrated that the application of both the cholinergic agonist CCh and KCl evoked a robust response in the hPSC-derived neurons, indicative of the opening of specific functional membrane channels resulting in an influx of fluorescent calcium dye. This was observed as in increase in fluorescence in individual neurons. (B) Quantification demonstrated the application of CCh lead to an average 47.5% ±7.9 increase in fluorescence levels and KCl resulted in a 67.3% ±8.1 increase above baseline (98 cells total, n = 6, SEM)]. (C) hPSC-derived neurons spontaneously released the neurotransmitter acetylcholine (ACh), which significantly increased in response to CCh, indicating specific cholinergic neuromodulatory ability and definitive proof of their cholinergic function (n = 4, SEM, two tailed *t*-test ** p = <0.01). (D) Whole-cell patch clamp electrophysiology was used to assess electrical firing properties of the hPSC-derived neurons, as shown in these representative voltage-responses to a 40 pA current injection (n = 5). Repetitive trains of action potentials were observed, which were completely blocked by the sodium channel blocker, TTX (500 nM). This was fully reversible following washout with aCSF. (E) Representative traces of spontaneous electrical firing activity. The neurons were voltage-clamped at −60 mV (n = 6). This was completely blocked by the application of TTX (500 nM). Subsequently, spontaneous activity was restored following washout with aCSF. (F) Summarized data of the mean frequency of spontaneous activity from differentiated neurons with control cells firing at a rate of 5.5 ± 0.3 Hz. TTX blocked all spontaneous activity and an aCSF washout restored this spontaneous activity a similar rate of 4.5 ± 0.4 Hz (n = 6 in all cases, SEM). (G) Immunoblot demonstrating expression of the synaptic marker Synapsin1 (isoforms 1a and 1b) on 8 week terminally differentiated NAS2 hiPS-derived cultures.

It has been reported by several studies that a naive neural differentiation system will produce derivatives with telencephalic identity, and this seems somewhat the 'default' neural fate of hPSCs (Watanabe et al., 2005; Gaspard et al., 2008; Li et al., 2009). However dorso-ventral fate is highly variable between protocols, and this is likely due to differentiation conditions generating their own intrinsic dorso-ventral induction (Bissonnette et al., 2011; Watanabe et al., 2005; Gaspard et al., 2008; Li et al., 2009; Danjo et al., 2011; Wataya et al., 2008). In terms of ventral forebrain, very high numbers of neural cells expressing markers of the ventral/basal forebrain, have only previously been achieved by the addition of specific doses of extrinsic SHH or other factors thought to influence this fate (Bissonnette et al., 2011; Watanabe et al., 2005; Gaspard et al., 2008; Li et al., 2009; Danjo et al., 2011; Nat et al., 2012; Ma et al., 2012). Interestingly, however several studies support our evidence for the early induction of hedgehog signaling in the EB, however this has never been utilized for bfCN differentiation. It has previously been demonstrated in two studies by Iacovitti et al., where exogenous ventralizing factors were absent from an EB-based protocol, which efficiently produced midbrain neurons with a ventral phenotype (Iacovitti et al., 2007; Cai et al., 2009). Furthermore, other studies generating non-neural derivatives also establish that EB formation does generate high levels of hedgehog signaling (Mfopou et al., 2007; Maye et al., 2000; Wu et al., 2010). Therefore, although the utilization of endogenous signaling pathways is not often reported for use in hPSC differentiation, it is clear that hPSCs have the ability to generate their own signals, and this does occur in the absence of over-riding high concentration signaling factors that are present in many protocols.

Expression of NKX2.1 and LHX8 in the NAdD generated NSCs was followed by expression of the bfCN transcription factor ISL1 upon terminal differentiation. Taken together this indicates that we were able to recapitulate embryonic events. Recently, two groups published findings indicating the generation of bfCNs from hES cells (Nilbratt et al., 2010;

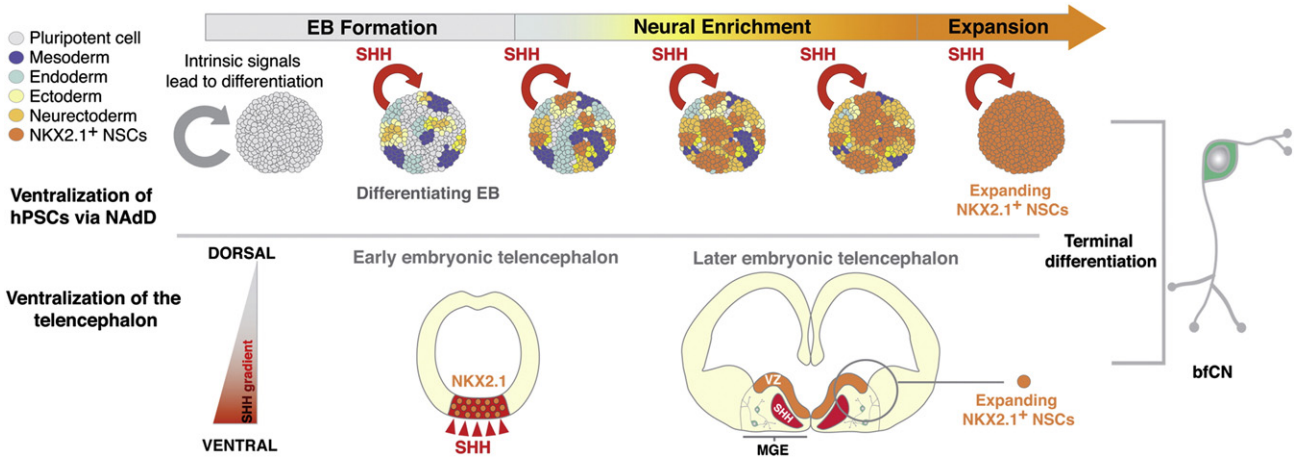

Figure 8 Schematic of the generation of ventral NKX2.1$^+$ NSCs, and bfCNs *via* NAdD of hPSCs in relation to events of the developing embryonic brain. EB formation with hPSCs generates intrinsic signaling which induces germ layer differentiation (upper panel). The 3D environment supports the secretion of SHH from the EB, resulting in ventralization of the neuroectoderm and generation of NSCs expressing the ventral telencephalic marker NKX2.1. This parallels events in the embryonic neural tube (lower panel) where SHH is initially secreted from mesendodermal tissue adjacent to the ventral neural tube, from which the ventral telencephalon develops. This induces the expression of SHH from the ventral neural tube itself, resulting in a dorso-ventral SHH gradient, with highest SHH levels required for ventral fate and this similarly results in rapid upregulation of NKX2.1. In the NAdD protocol, the enrichment stage followed by expansion in the presence of mitogens results in non-adherent neurospheres, made up of an almost pure population of expanding NKX2.1$^+$ NSCs. They are therefore equivalent to the progenitors in the ventricular zone of the embryonic MGE within the basal forebrain. Similarly upon terminal differentiation the NSCs efficiently generate bfCNs.

Bissonnette et al., 2011). In both cases bfCN differentiation was dependent on exposing hES cells to known factors required in the developing basal forebrain either by ectopic application in the differentiation media or by over-expression (Nilbratt et al., 2010; Bissonnette et al., 2011). An accurate developmental model of any neuronal population affected by neurodegeneration is key to therapeutic progress, as in terms of neuroprotection, regeneration or replacement, it is crucial that we understand the factors required for cell differentiation and survival (Nat and Dechant, 2011; Liu, 2011). We therefore conclude that our NAdD protocol, in the absence of exogenous factors, better recapitulates developmental events in the basal forebrain, and thus serves as an accurate model for studying the development of bfCNs.

In this study hPSC-derived bfCNs were generated *via* an expandable NSC intermediate, which maintained the desired basal forebrain progenitor phenotype, and neurogenic capacity even after long-term expansion in culture. This scalability is a required feature of any cell type to be used in regenerative medicine. Whether it is for application in cell replacement or for the development of novel drug therapies, both require high numbers of cells. This, taken together with the absence of extrinsic factors in our protocol reduces the cost of generating high numbers of bfCNs, which is crucial for any large-scale applications, such as drug screening.

Further examination of the hPSC-derived bfCN phenotype revealed a number of characteristics crucial for a model of bfCNs in AD. They expressed p75^{NTR}, which is involved in the development and survival of bfCNs, and significantly has also been linked to AD pathology (Allen and Dawbarn, 2006).

Furthermore we were able to show long-term survival and *in vivo* differentiation of hPSC-derived bfCNs, suggesting they were able to integrate into the adult basal forebrain. However, to what extent remains unclear and further work is required to determine if the hPSC-derived cells were able to form functional synapses with *in vivo* neurons.

In addition the hPSC-derived bfCNs had a mature electrophysiological profile, demonstrating an action potential through depolarization and also spontaneous electrical activity. In context of their use as a model of the basal forebrain cholinergic system, it is well established that AD pathology has a complex effect on the cholinergic neuromodulatory role of bfCNs and their electrical function, resulting in both hypo- and hyperactivity at synapses (Huang and Mucke, 2012). This is of major interest to the AD research field as it is accepted that synaptic dysfunction is the major cause of cognitive decline, and therefore crucial if they are to be used as a model of AD pathology, much of which is only applicable to mature neurons.

In conclusion, we have demonstrated a novel protocol for the efficient generation of bfCNs from hPSCs, *via* an expandable NSC intermediate, which recapitulates basal forebrain development. This replication of *in vivo* human bfCN differentiation provides a valuable *in vitro* model for the development of this population, which is otherwise inaccessible. The mature derivatives of this protocol are an accurate recapitulation of adult bfCNs, and therefore an excellent model for the study of the human basal forebrain cholinergic system, for the development of novel therapeutics targeted towards AD (Liu, 2011). Finally, this is the first incidence of cholinergic differentiation from hiPSCs and therefore the first method to provide the opportunity to examine the specific effects of AD on patient derived bfCNs.

Supplementary data to this article can be found online at http://dx.doi.org/10.1016/j.scr.2013.08.002.

Acknowledgments

This work was funded by the James Tudor Foundation, BRACE, Alzheimer's Research UK and the BBSRC.

References

Allen, S.J., Dawbarn, D., 2006. Clinical relevance of the neurotrophins and their receptors. Clin. Sci. (Lond.) 110 (2), 175–191.

Anderson, L., Burnstein, R.M., He, X., Luce, R., Furlong, R., Foltynie, T., et al., 2007. Gene expression changes in long term expanded human neural progenitor cells passaged by chopping lead to loss of neurogenic potential *in vivo*. Exp. Neurol. 204 (2), 512–524.

Bissonnette, C.J., Lyass, L., Bhattacharyya, B.J., Belmadani, A., Miller, R.J., Kessler, J.A., 2011. The controlled generation of functional Basal forebrain cholinergic neurons from human embryonic stem cells. Stem Cells 29 (5), 802–811.

Briscoe, J., Ericson, J., 1999. The specification of neuronal identity by graded Sonic Hedgehog signalling. Semin. Cell Dev. Biol. 10 (3), 353–362.

Cai, J., Donaldson, A., Yang, M., German, M.S., Enikolopov, G., Iacovitti, L., 2009. The role of Lmx1a in the differentiation of human embryonic stem cells into midbrain dopamine neurons in culture and after transplantation into a Parkinson's disease model. Stem Cells 27 (1), 220–229.

Caldwell, M.A., He, X., Wilkie, N., Pollack, S., Marshall, G., Wafford, K.A., et al., 2001. Growth factors regulate the survival and fate of cells derived from human neurospheres. Nat. Biotechnol. 19 (5), 475–479.

Carpenter, M.K., Cui, X., Hu, Z.Y., Jackson, J., Sherman, S., Seiger, A., et al., 1999. *In vitro* expansion of a multipotent population of human neural progenitor cells. Exp. Neurol. 158 (2), 265–278.

Chambers, S.M., Fasano, C.A., Papapetrou, E.P., Tomishima, M., Sadelain, M., Studer, L., 2009. Highly efficient neural conversion of human ES and iPS cells by dual inhibition of SMAD signaling. Nat. Biotechnol. 27 (3), 275–280.

Coulson, E.J., May, L.M., Sykes, A.M., Hamlin, A.S., 2009. The role of the p75 neurotrophin receptor in cholinergic dysfunction in Alzheimer's disease. Neuroscientist 15 (4), 317–323.

Danjo, T., Eiraku, M., Muguruma, K., Watanabe, K., Kawada, M., Yanagawa, Y., et al., 2011. Subregional specification of embryonic stem cell-derived ventral telencephalic tissues by timed and combinatory treatment with extrinsic signals. J. Neurosci. 31 (5), 1919–1933.

Davies, P., Maloney, A.J., 1976. Selective loss of central cholinergic neurons in Alzheimer's disease. Lancet 2 (8000), 1403.

Devine, M.J., Ryten, M., Vodicka, P., Thomson, A.J., Burdon, T., Houlden, H., et al., 2011. Parkinson's disease induced pluripotent stem cells with triplication of the alpha-synuclein locus. Nat. Commun. 2, 440.

Echelard, Y., Epstein, D.J., St-Jacques, B., Shen, L., Mohler, J., McMahon, J.A., et al., 1993. Sonic hedgehog, a member of a family of putative signaling molecules, is implicated in the regulation of CNS polarity. Cell 75 (7), 1417–1430.

Elkabetz, Y., Panagiotakos, G., Al Shamy, G., Socci, N.D., Tabar, V., Studer, L., 2008. Human ES cell-derived neural rosettes reveal a functionally distinct early neural stem cell stage. Genes Dev. 22 (2), 152–165.

Elshatory, Y., Gan, L., 2008. The LIM-homeobox gene Islet-1 is required for the development of restricted forebrain cholinergic neurons. J. Neurosci. 28 (13), 3291–3297.

Ericson, J., Muhr, J., Placzek, M., Lints, T., Jessell, T.M., Edlund, T., 1995a. Sonic hedgehog induces the differentiation of ventral forebrain neurons: a common signal for ventral patterning within the neural tube. Cell 81 (5), 747–756.

Ericson, J., Muhr, J., Jessell, T.M., Edlund, T., 1995b. Sonic hedgehog: a common signal for ventral patterning along the rostrocaudal axis of the neural tube. Int. J. Dev. Biol. 39 (5), 809–816.

Everitt, B.J., Robbins, T.W., 1997. Central cholinergic systems and cognition. Annu. Rev. Psychol. 48, 649–684.

Flandin, P., Kimura, S., Rubenstein, J.L., 2010. The progenitor zone of the ventral medial ganglionic eminence requires Nkx2-1 to generate most of the globus pallidus but few neocortical interneurons. J. Neurosci. 30 (8), 2812–2823.

Fragkouli, A., Hearn, C., Errington, M., Cooke, S., Grigoriou, M., Bliss, T., et al., 2005. Loss of forebrain cholinergic neurons and impairment in spatial learning and memory in LHX7-deficient mice. Eur. J. Neurosci. 21 (11), 2923–2938.

Gaspard, N., Bouschet, T., Hourez, R., Dimidschstein, J., Naeije, G., van den Ameele, J., et al., 2008. An intrinsic mechanism of corticogenesis from embryonic stem cells. Nature 455 (7211), 351–357.

Griguoli, M., Cherubini, E., 2012. Regulation of hippocampal inhibitory circuits by nicotinic acetylcholine receptors. J. Physiol. 590 (Pt 4), 655–666.

Gunhaga, L., Jessell, T.M., Edlund, T., 2000. Sonic hedgehog signaling at gastrula stages specifies ventral telencephalic cells in the chick embryo. Development 127 (15), 3283–3293.

Han, S.S., Williams, L.A., Eggan, K.C., 2011. Constructing and deconstructing stem cell models of neurological disease. Neuron 70 (4), 626–644.

Holtzman, D.M., Morris, J.C., Goate, A.M., 2011. Alzheimer's disease: the challenge of the second century. Sci. Transl. Med. 3 (77), 77sr1.

Huang, Y., Mucke, L., 2012. Alzheimer mechanisms and therapeutic strategies. Cell 148 (6), 1204–1222.

Iacovitti, L., Donaldson, A.E., Marshall, C.E., Suon, S., Yang, M., 2007. A protocol for the differentiation of human embryonic stem cells into dopaminergic neurons using only chemically defined human additives: studies *in vitro* and *in vivo*. Brain Res. 1127 (1), 19–25.

Joannides, A.J., Fiore-Heriche, C., Battersby, A.A., Athauda-Arachchi, P., Bouhon, I.A., Williams, L., et al., 2007. A scaleable and defined system for generating neural stem cells from human embryonic stem cells. Stem Cells 25 (3), 731–737.

Johnson, M.A., Weick, J.P., Pearce, R.A., Zhang, S.C., 2007. Functional neural development from human embryonic stem cells: accelerated synaptic activity *via* astrocyte coculture. J. Neurosci. 27 (12), 3069–3077.

Li, X.J., Zhang, X., Johnson, M.A., Wang, Z.B., Lavaute, T., Zhang, S.C., 2009. Coordination of sonic hedgehog and Wnt signaling determines ventral and dorsal telencephalic neuron types from human embryonic stem cells. Development 136 (23), 4055–4063.

Liu, H., Zhang, S.C., 2011. Specification of neuronal and glial subtypes from human pluripotent stem cells. Cell. Mol. Life Sci.

Ma, L., Hu, B., Liu, Y., Vermilyea, S.C., Liu, H., Gao, L., et al., 2012. Human embryonic stem cell-derived GABA neurons correct locomotion deficits in quinolinic acid-lesioned mice. Cell Stem Cell 10 (4), 455–464.

Marin, O., Anderson, S.A., Rubenstein, J.L., 2000. Origin and molecular specification of striatal interneurons. J. Neurosci. 20 (16), 6063–6076.

Martin, G.R., Evans, M.J., 1975. Differentiation of clonal lines of teratocarcinoma cells: formation of embryoid bodies *in vitro*. Proc. Natl. Acad. Sci. U. S. A. 72 (4), 1441–1445.

Masoudi, R., Ioannou, M.S., Coughlin, M.D., Pagadala, P., Neet, K.E., Clewes, O., et al., 2009. Biological activity of nerve growth

factor precursor is dependent upon relative levels of its receptors. J. Biol. Chem. 284 (27), 18424–18433.

Maye, P., Becker, S., Kasameyer, E., Byrd, N., Grabel, L., 2000. Indian hedgehog signaling in extraembryonic endoderm and ectoderm differentiation in ES embryoid bodies. Mech. Dev. 94 (1–2), 117–132.

Mfopou, J.K., De Groote, V., Xu, X., Heimberg, H., Bouwens, L., 2007. Sonic hedgehog and other soluble factors from differentiating embryoid bodies inhibit pancreas development. Stem Cells 25 (5), 1156–1165.

Nat, R., Dechant, G., 2011. Milestones of directed differentiation of mouse and human embryonic stem cells into telencephalic neurons based on neural development *in vivo*. Stem Cells Dev. 20 (6), 947–958.

Nat, R., Salti, A., Suciu, L., Strom, S., Dechant, G., 2012. Pharmacological modulation of the hedgehog pathway differentially affects dorsal/ventral patterning in mouse and human embryonic stem cell models of telencephalic development. Stem Cells Dev. 21 (7), 1016–1046.

Nilbratt, M., Porras, O., Marutle, A., Hovatta, O., Nordberg, A., 2010. Neurotrophic factors promote cholinergic differentiation in human embryonic stem cell-derived neurons. J. Cell. Mol. Med. 14 (6B), 1476–1484.

Pera, E.M., Kessel, M., 1997. Patterning of the chick forebrain anlage by the prechordal plate. Development 124 (20), 4153–4162.

Ross, P.J., Suhr, S.T., Rodriguez, R.M., Chang, E.A., Wang, K., Siripattarapravat, K., et al., 2010. Human-induced pluripotent stem cells produced under xeno-free conditions. Stem Cells Dev. 19 (8), 1221–1229.

Shimamura, K., Rubenstein, J.L., 1997. Inductive interactions direct early regionalization of the mouse forebrain. Development 124 (14), 2709–2718.

Shimamura, K., Hartigan, D.J., Martinez, S., Puelles, L., Rubenstein, J.L., 1995. Longitudinal organization of the anterior neural plate and neural tube. Development 121 (12), 3923–3933.

Sussel, L., Marin, O., Kimura, S., Rubenstein, J.L., 1999. Loss of Nkx2.1 homeobox gene function results in a ventral to dorsal molecular respecification within the basal telencephalon: evidence for a transformation of the pallidum into the striatum. Development 126 (15), 3359–3370.

Svendsen, C.N., ter Borg, M.G., Armstrong, R.J., Rosser, A.E., Chandran, S., Ostenfeld, T., et al., 1998. A new method for the rapid and long term growth of human neural precursor cells. J. Neurosci. Methods 85 (2), 141–152.

Vallier, L., Reynolds, D., Pedersen, R.A., 2004. Nodal inhibits differentiation of human embryonic stem cells along the neuroectodermal default pathway. Dev. Biol. 275 (2), 403–421.

Vescovi, A.L., Parati, E.A., Gritti, A., Poulin, P., Ferrario, M., Wanke, E., et al., 1999. Isolation and cloning of multipotential stem cells from the embryonic human CNS and establishment of transplantable human neural stem cell lines by epigenetic stimulation. Exp. Neurol. 156 (1), 71–83.

Watanabe, K., Kamiya, D., Nishiyama, A., Katayama, T., Nozaki, S., Kawasaki, H., et al., 2005. Directed differentiation of telencephalic precursors from embryonic stem cells. Nat. Neurosci. 8 (3), 288–296.

Watanabe, K., Ueno, M., Kamiya, D., Nishiyama, A., Matsumura, M., Wataya, T., et al., 2007. A ROCK inhibitor permits survival of dissociated human embryonic stem cells. Nat. Biotechnol. 25 (6), 681–686.

Wataya, T., Ando, S., Muguruma, K., Ikeda, H., Watanabe, K., Eiraku, M., et al., 2008. Minimization of exogenous signals in ES cell culture induces rostral hypothalamic differentiation. Proc. Natl. Acad. Sci. U. S. A. 105 (33), 11796–11801.

Whiting, P.J., Lindstrom, J.M., 1988. Characterization of bovine and human neuronal nicotinic acetylcholine receptors using monoclonal antibodies. J. Neurosci. 8 (9), 3395–3404.

Wu, P., Tarasenko, Y.I., Gu, Y., Huang, L.Y., Coggeshall, R.E., Yu, Y., 2002. Region-specific generation of cholinergic neurons from fetal human neural stem cells grafted in adult rat. Nat. Neurosci. 5 (12), 1271–1278.

Wu, S.M., Choo, A.B., Yap, M.G., Chan, K.K., 2010. Role of Sonic hedgehog signaling and the expression of its components in human embryonic stem cells. Stem Cell Res. 4 (1), 38–49.

Zhao, Y., Marin, O., Hermesz, E., Powell, A., Flames, N., Palkovits, M., et al., 2003. The LIM-homeobox gene Lhx8 is required for the development of many cholinergic neurons in the mouse forebrain. Proc. Natl. Acad. Sci. U. S. A. 100 (15), 9005–9010.

Zoukhri, D., Kublin, C.L., 2002. Impaired neurotransmission in lacrimal and salivary glands of a murine model of Sjogren's syndrome. Adv. Exp. Med. Biol. 506 (Pt B), 1023–1028.